Hindawi
Mathematical Problems in Engineering
Volume 2019, Article ID 5794791, 8 pages
https://doi.org/10.1155/2019/5794791

Research Article

Coherent Signal Parameter Estimation by Exploiting Decomposition of Tensors

Long Liu,[1] **Ling Wang**,[1] **Yuexian Wang**,[2] **Jian Xie**,[1] **and Zhaolin Zhang**[1]

[1]*School of Electronics and Information, Northwestern Polytechnical University, Xi'an 710072, China*
[2]*School of Electrical and Electronics Engineering, The University of Adelaide, Adelaide, SA 5005, Australia*

Correspondence should be addressed to Ling Wang; lingwang@nwpu.edu.cn

Received 15 July 2019; Accepted 1 November 2019; Published 13 November 2019

Academic Editor: Alessio Gizzi

The problem of parameter estimation of coherent signals impinging on an array with vector sensors is considered from a new perspective by means of the decomposition of tensors. Signal parameters to be estimated include the direction of arrival (DOA) and the state of polarization. In this paper, mild deterministic conditions are used for canonical polyadic decomposition (CPD) of the tensor-based signal model; i.e., the factor matrices can be recovered, as long as the matrices satisfy the requirement that at least one is full column rank. In conjoint with the estimation of signal parameters via the algebraic method, the DOAs and polarization parameters of coherent signals can be resolved by virtue of the first and second factor matrices. Hereinto, the key innovation of the proposed approach is that the proposed approach can effectively estimate the coherent signal parameters without sacrificing the array aperture. The superiority of the proposed algorithm is shown by comparing with the algorithms based on higher order singular value decomposition (HOSVD) and Toeplitz matrix. Theoretical and numerical simulations demonstrate the effectiveness of the proposed approach.

1. Introduction

The problem of parameter estimation for coherent signals is encountered in a variety of signal processing applications including wireless communication, satellite navigation, and radar. Generally, the signal covariance matrix must be full rank for the subspace-based high-resolution estimation approaches such as multiple signal classification (MUSIC) and estimation of signal parameters via rotational invariance techniques (ESPRITs). However, there is also a fact that cannot be ignored; that is, the presence of the coherent signals can cause the rank loss of the covariance matrix. Under such circumstances, the spatial smoothing technique and its derivative algorithms [1–5] are commonly used as a conventional solution to this problem. According to previous research studies, these approaches have been proved to play an important role in eliminating the rank loss of the covariance matrix, but they are not flawless because an unignorable large aperture loss appears under these approaches as well, degrading the accuracy of parameter estimation. Apart from these approaches, the approaches of parameter estimation for coherent signals based on the Toeplitz matrix signal model have received considerable attention and developments because the rank of the Toeplitz matrix is only related to the DOA of signals and cannot be affected by the coherency between them [6–10]. In addition, in the context of underwater environment and target imaging, the coherent signal analysis methods proposed in [11, 12] are also worthy of attention. For all the approaches mentioned above, they share a common feature that the process of parameter estimation is based on matrix operations.

However, the matrix can only reflect the two-dimensional characteristics of the signal. For multidimensional signals, stacking dimensions into one highly structured matrix can effectively improve the accuracy of parameter estimation. In [13], the measurement tensor has been defined, and the estimation of the subspace through higher order singular value decomposition (HOSVD) has

been proposed. Similarly, the HOSVD-based algorithms have been studied to improve the performance of parameter estimation in [14–17]. However, in order to achieve the parameter estimation of coherent signals, smoothing for tensor is unavoidable in terms of the HOSVD-based algorithms, which will also lead to the sacrifice of array aperture.

Recently, parameter estimation methods by exploiting the canonical polyadic decomposition (CPD) of tensor, which is a minimal decomposition into a sum of rank-1 tensors, have been studied in [18–21]. One common feature of the existing tensor CPD-based parameter estimation methods is that they are all directed to noncoherent signal models. In this paper, we will study the CPD-based approach of parameter estimation under the condition that at least two signals satisfy the coherent premise.

Here, we present a signal model based on the third-order tensor, with three dimensions corresponding to the temporal, spatial, and polarized information of the signal. Furthermore, the mild deterministic conditions [22] are used for CPD of the tensor-based signal model; i.e., as long as the coherent signals comply with any one of the spatial and polarized diversities, the proposed approach can effectively estimate the parameters of the coherent signals. The parameters to be estimated mainly include the DOA and polarization parameters delivered by the signal. Computer results are reported as a function of the signal-to-noise ratio (SNR), in comparison to the advanced subspace-based approaches. In addition, the estimation accuracy of polarized parameters is also studied with respect to the different SNR values.

The rest of this paper is organized as follows: Section 2 derives the tensor-based signal model, followed by the proposed algorithm for extracting the signal parameters in Section 3. Meanwhile, numerical simulations are provided in Section 5. Finally, the last part of the paper will present our concluding remarks. Table 1 summarizes the algebra notations involved in this paper.

Table 1: Algebra notations.

ν	Scalar ν
$\mathbf{v}$	Vector $\mathbf{v}$
$\mathbf{A}$	Matrix $\mathbf{A}$
$\mathscr{A}$	Tensor $\mathscr{A}$
$\mathbb{R}$	Real number field
$\mathbb{C}$	Complex number field
$\mathbf{A}^T$	Transpose of A
$\mathbf{A}^H$	Conjugate transpose of A
$\mathscr{A} \circledcirc \mathscr{B}$	Outer product between $\mathscr{A}$ and $\mathscr{B}$
$\mathbf{A} \otimes \mathbf{B}$	Kronecker product between $\mathbf{A}$ and $\mathbf{B}$
$\mathbf{A} \odot \mathbf{B}$	Khatri–Rao product between $\mathbf{A}$ and $\mathbf{B}$
$\mathbf{A} \circ \mathbf{B}$	Hadamard product between $\mathbf{A}$ and $\mathbf{B}$
$r_{\mathbf{A}}$	Rank of the matrix $\mathbf{A}$
$\|\mathbf{A}\|_F$	Frobenius norm of A
$\|\mathbf{v}\|_2$	2-norm of $\mathbf{v}$

2. Signal Model

Let $\theta \in [0, 2\pi)$ and $\phi \in [0, \pi]$ serve as the indications of the azimuth angle and the elevation angle. Set the number of electromagnetic (EM) vector sensors in the array as L, and the components measured by an EM vector sensor are indexed as $1, \ldots, J$ separately. The spatial steering vector for the array with DOA (θ, ϕ) is given by

$$\mathbf{a}^s(\theta, \phi) = \left[e^{-i2\pi f_1}, \ldots, e^{-i2\pi f_L}\right]^T, \tag{1}$$

where $f_l = \mathbf{b}_l^T \epsilon / \lambda$, $\epsilon = -[\sin\phi_r \cos\theta_r \;\; \sin\phi_r \sin\theta_r \cos\phi_r]^T$, and $\mathbf{b}_l \in \mathbb{R}^3$ indicates the spatial location of the lth sensor, $l = 1, \ldots, L$. Let $\Psi = (\theta, \phi, \gamma, \eta)$ indicate the spatial-polarization parameter, where $\gamma \in [0, \pi/2]$ symbolizes the polarization auxiliary angle and $\eta \in [-\pi, \pi)$ symbolizes the polarization-phase difference. The polarization steering vector can be denoted as

$$\mathbf{a}^p(\Psi) = \mathscr{B} \underbrace{\begin{bmatrix} -\sin\theta & \cos\phi\cos\theta \\ \cos\theta & \cos\phi\sin\theta \\ 0 & -\sin\phi \\ \cos\phi\cos\theta & \sin\theta \\ \cos\phi\sin\theta & -\cos\theta \\ -\sin\phi & 0 \end{bmatrix}}_{\Xi_{\theta,\phi}} \mathbf{h}_{\gamma,\eta}, \tag{2}$$

where $\mathbf{h}_{\gamma,\eta} = [\cos\gamma \;\; \sin\gamma e^{i\eta}]^T$ and $\mathscr{B} \in \mathbb{R}^{J\times 6}$ is defined as the polarization selection matrix for the EM vector sensor. In particular, for the complete EM vector sensor, the polarization selection matrix is represented as $\mathscr{B} = \mathbf{I}_{6\times 6}$ and $\mathscr{B} = [\mathbf{I}_{3\times 3}, 0_{3\times 3}]$ belongs to the three dipoles, in which $\mathbf{I}$ symbolizes the unit matrix. The spatial-polarization steering vector of the signal with the spatial-polarization parameter Ψ can be further given by

$$\mathbf{a}(\Psi) = \mathbf{a}^s(\theta, \phi) \otimes \mathbf{a}^p(\Psi). \tag{3}$$

Hereby, the R signals with the complex amplitudes $\{s_r(k), r = 1, \ldots, R\}$ are assumed to be received by the array. Furthermore, assume that the first R_1 signals are coherent and the last R_2 signals are noncoherent, but all the signals are in cofrequency, where $R_1 + R_2 = R$. Construct the following equation to represent the vector output of the array at the instant t_k:

$$\mathbf{y}(k) = \sum_{r=1}^{R} \mathbf{a}(\Psi_r) s_r(k) + \mathbf{n}(k), \tag{4}$$

where the additive prewhitening noise $\mathbf{n}(k)$ is assumed to have a Gaussian complex circular. In order to better distinguish the multidomain diversities of the signal, we perform tensorization on (3) so that the multidomain diversities of the signal caters to the multidimensional nature of the tensor, and then the following representation is obtained:

$$\widehat{A}(\Psi) = \mathbf{a}^p(\Psi) \circledcirc \mathbf{a}^s(\theta, \phi). \tag{5}$$

Furthermore, the tensor output of the consecutive K snapshots for the array can be modeled as

$$\begin{aligned}\mathcal{Y} &= \sum_{r=1}^{R} \widehat{A}(\Psi_r) \circledcirc \mathbf{s}_r + \mathcal{N} \\ &= \sum_{r=1}^{R} \mathbf{a}^p(\Psi_r) \circledcirc \mathbf{a}^s(\theta_r, \phi_r) \circledcirc \mathbf{s}_r + \mathcal{N},\end{aligned} \tag{6}$$

where $\mathcal{Y} \in \mathbb{C}^{J\times L\times K}$ and $\mathbf{s}_r = [s_r(1), \ldots, s_r(K)]$. In addition, the noise tensor $\mathcal{N} \in \mathbb{C}^{J\times L\times K}$ is yielded by tensorization with respect to the noise matrix $\mathbf{N} = [\mathbf{n}(1), \ldots, \mathbf{n}(k)]$.

3. The Proposed Approach

Let $\mathcal{T} = \sum_{r=1}^{R} \mathbf{a}_r^p \circledcirc \mathbf{a}_r^s \circledcirc \mathbf{s}_r$. Thereby, equation (6) can be expressed as

$$\mathcal{Y} = \mathcal{T} + \mathcal{N}. \tag{7}$$

Considering that $\mathbf{a}_r^p \in \mathbb{C}^J$, $\mathbf{a}_r^s \in \mathbb{C}^L$, and $\mathbf{s}_r \in \mathbb{C}^K$ are nonzero vectors, tensor $\mathcal{S}_r = \mathbf{a}_r^p \circledcirc \mathbf{a}_r^s \circledcirc \mathbf{s}_r$ is the rank-1 tensor. If the number R of the rank-1 terms in $\mathcal{T}$ is minimal, then $\mathcal{T} = \sum_r^R \mathcal{S}_r$ is called the CPD of $\mathcal{T}$ and R is called the rank of $\mathcal{T}$ (denoted by $r_{\mathcal{T}}$). Since the addition of noise component $\mathcal{N}$, the structure of the tensor $\mathcal{Y}$ is significantly different from the structure of the tensor $\mathcal{T}$. Herein, we are not going to talk about the structure of the tensor $\mathcal{Y}$, but instead regard it as the rank R tensor and decompose it. Furthermore, the estimation of the factor matrices can be obtained.

3.1. Construction of Intermediate Tensor. The CPD of $\mathcal{Y}$ can be expressed as

$$\mathcal{Y} = \sum_{r=1}^{R} \mathbf{a}_r \circledcirc \mathbf{b}_r \circledcirc \mathbf{c}_r, \tag{8}$$

where $\mathbf{a}_r \in \mathbb{C}^J$, $\mathbf{b}_r \in \mathbb{C}^L$, and $\mathbf{c}_r \in \mathbb{C}^K$. Let $\mathbf{A} = [\mathbf{a}_1, \ldots, \mathbf{a}_R] \in \mathbb{C}^{J\times R}$, $\mathbf{B} = [\mathbf{b}_1, \ldots, \mathbf{b}_R] \in \mathbb{C}^{L\times R}$, and $\mathbf{C} = [\mathbf{c}_1, \ldots, \mathbf{c}_R] \in \mathbb{C}^{K\times R}$. We can also write (8) as $\mathcal{Y} = [\mathbf{A}, \mathbf{B}, \mathbf{C}]_R$, where $\mathbf{A}$, $\mathbf{B}$, and $\mathbf{C}$ are called the first, second, and third factor matrix of $\mathcal{Y}$, respectively. Again, we can write $\mathcal{T}$ as $\mathcal{T} = [\mathbf{A}_p, \mathbf{A}_s, \mathbf{S}]_R$, where $\mathbf{A}_p = [\mathbf{a}^p(\Psi_1), \ldots, \mathbf{a}^p(\Psi_R)]$, $\mathbf{A}_s = [\mathbf{a}^s(\theta_1, \phi_1), \ldots, \mathbf{a}^s(\theta_R, \phi_R)]$, and $\mathbf{S} = [\mathbf{s}_1, \ldots, \mathbf{s}_R]$. Furthermore, we call that the CPD of the tensor is unique when it is the only subject to the trivial indeterminacies, in which the factor matrices can be arbitrarily permuted and the vectors belonging to any factor matrix can be arbitrarily scaled. Obviously, the factor matrices of $\mathcal{Y}$ and the factor matrices of $\mathcal{T}$ do not satisfy the above indeterminacies due to the presence of the noise. Therefore, $\mathbf{A}$, $\mathbf{B}$, and $\mathbf{C}$ are considered as the estimated values of $\mathbf{A}_p$, $\mathbf{A}_s$, and $\mathbf{S}$, respectively.

Herein, we only consider the algebraic algorithm for CPD under the condition that at least one factor matrix of $\mathcal{T}$ has full column rank. That is to say, in the tensor $\mathcal{Y}$, at least one factor matrix contains highly collinear vectors due to the presence of noise disturbances. In order to adapt to the analysis of the coherent signal tensor model, we extend Theorem 2 and Theorem 8 in [22]. The following theorem can be obtained.

Theorem 1. *Let* $\mathcal{T} = [\mathbf{A}_p, \mathbf{A}_s, \mathbf{S}]_R$ *and* $r_{\mathbf{A}_s} = L = R$, $i \geq 0$ *Assume that*

$$\dim\left(\ker\left(\mathbf{R}_{2,i}(\mathcal{T})\right) \cap S^{2+i}\left(\mathbb{C}^{L^{2+i}}\right)\right) = R. \tag{9}$$

Then, $r_{\mathcal{T}} = R$, *and the CPD of* $\mathcal{T}$ *is unique. In addition, the CPD of* $\mathcal{T}$ *can be obtained algebraically. Under this premise, the proposed algorithm can achieve a unique decomposition of the tensor* $\mathcal{Y}$.

Matrix $\mathbf{R}_{m,i}(\mathcal{T})$ is defined in Appendix A. $S^{m+i}(\mathbb{C}^{L^{m+i}}) \subset \mathbb{C}^{L^{m+i}}$ denotes the subspace spanned by all vectors of the form $\mathbf{x} \otimes \cdots \otimes \mathbf{x}$, where $\mathbf{x} \in \mathbb{C}^L$ is repeated $m + i$ times.

We hereby execute the decomposition of the tensor-based signal model to obtain the factor matrices, which are then used to extract the parameters of the signals. Assume that $r_{\mathbf{B}} = L = R$. First of all, the $C_J^m C_K^m \times C_{L+m-1}^m$ matrix $\mathbf{Q}_m(\mathcal{Y})$ needs to be built, and the $(l_1, \ldots, l_m)$-th column of the matrix $\mathbf{Q}_m(\mathcal{Y})$ can be obtained as follows:

$$[\mathbf{Q}_m(\mathcal{Y})]_{:,(l_1,\ldots,l_m)} = \mathrm{vec}\left(\mathcal{F}_{m-1}\left(\mathbf{Y}_{l_1}, \ldots, \mathbf{Y}_{l_m}\right)\right), \tag{10}$$

where $(l_1, \ldots, l_m) \in Q_L^m$, $\mathbf{Y}_1, \ldots, \mathbf{Y}_L \in \mathbb{C}^{J\times K}$ represents the frontal slices of the tensor $\mathcal{Y}$, and $Q_L^m = \{(l_1, \ldots, l_m) : 1 \leq l_1 \leq l_2 \leq \ldots \leq l_m \leq L\}$. An equation for the polarized compound matrix $\mathcal{F}_{m-1}(\mathbf{Y}_1, \ldots, \mathbf{Y}_m)$ can be defined as

$$\begin{aligned}\mathcal{F}_{m-1}(\mathbf{Y}_1, \ldots, \mathbf{Y}_m) = \sum_{k=1}^{m} (-1)^{m-k} \sum_{1\leq i_1<i_2\cdots<i_k\leq m} \\ \cdot \mathscr{C}_m\left(\mathbf{Y}_{i_1} + \mathbf{Y}_{i_2} + \cdots + \mathbf{Y}_{i_k}\right),\end{aligned} \tag{11}$$

where the m-th compound matrix $\mathscr{C}_m(\mathbf{X})$ of a given matrix $\mathbf{X}$ can be obtained from Appendix B.

Subsequently, how to get the vectors $\widehat{w}_1, \ldots, \widehat{w}_{C_R^{L-1}}$ from the matrix $\mathbf{Q}_m(\mathcal{Y})$ is the focus of this paper. In the absence of noise, for the tensor $\mathcal{T}$, as described in [23], vectors $\widehat{w}_1, \ldots, \widehat{w}_{C_R^{L-1}}$ form a basis of $\ker(\mathbf{Q}_m(\mathcal{T}))$. Combining the construction process of the matrix $\mathbf{Q}_m(\mathcal{T})$, the vector $\widehat{w}_i$ satisfying $\mathbf{Q}_m(\mathcal{T})\widehat{w}_i = 0$ has the following structural features:

$$\begin{aligned}\widehat{w}_{i,1:a} &= \left[\widehat{w}_{i,1}, \ldots, \widehat{w}_{i,a}\right]^T, \\ \widehat{w}_{i,a+1:C_{L+m-1}^m} &= \left[0, \ldots, \widehat{w}_{i,a+i}, \ldots, 0\right]^T,\end{aligned} \tag{12}$$

where $i \in [1, C_R^{L-1}]$, $a = C_{L+m-1}^m - C_R^{L-1}$, and the element $\widehat{w}_{i,a+i}$ is constant 1. Similarly, we can also write $\mathbf{Q}_m(\mathcal{T})$ as $\mathbf{Q}_m(\mathcal{T}) = [\mathbf{Q}_m^1(\mathcal{T}), \mathbf{Q}_m^2(\mathcal{T})]$, where the submatrices $\mathbf{Q}_m^1(\mathcal{T})$ and $\mathbf{Q}_m^2(\mathcal{T})$ contain the first a columns and the last C_R^{L-1} columns of $\mathbf{Q}_m(\mathcal{T})$, respectively. Therefore, the following equation is established:

$$\mathbf{Q}_m^1(\mathcal{T})\widehat{w}_{i,1:a} + \left[\mathbf{Q}_m^2(\mathcal{T})\right]_{:,i} = 0, \tag{13}$$

where $[\mathbf{Q}_m^2(\mathcal{T})]_{:,i}$ represents the ith column of the submatrix $\mathbf{Q}_m^2(\mathcal{T})$.

However, the vectors $\widehat{w}_1, \ldots, \widehat{w}_{C_R^{L-1}}$ cannot be obtained by solving the basis of the matrix $\ker(\mathbf{Q}_m(\mathcal{Y}))$ due to the presence of noise. Inspired by (12) and (13) summarized in this paper, an optimization problem model is established as follows:

$$\min_{\widehat{w}_{i,1:a}} \left\| \mathbf{Q}_m^1(\mathscr{Y})\widehat{w}_{i,1:a} + \left[\mathbf{Q}_m^2(\mathscr{Y})\right]_{:,i} \right\|_2. \tag{14}$$

Herein, the alternating least squares (ALS) method is used to solve the optimization problem (14), and then the vectors $\widehat{w}_1, \ldots, \widehat{w}_{C_R^{L-1}}$ can be obtained according to (12).

Let $\left\{\mathbf{e}_j^L\right\}_{j=1}^L$ denotes the canonical basis of $\mathbb{R}^L$, and then $\left\{\mathbf{e}_{j_1}^L \otimes \cdots \otimes \mathbf{e}_{j_m}^L\right\}_{(j_1,\ldots,j_m)\in R_L^m}$ is the canonical basis of $\mathbb{R}^{L^m}$, $R_L^m = \{(j_1, \ldots, j_m) : j_1, \ldots, j_m \in \{1, \ldots, L\}\}$. The symmetrizer π_S on the space $\mathbb{R}^{L^m}$ can be denoted as

$$\pi_S\left(\mathbf{e}_{j_1}^L \otimes \ldots \otimes \mathbf{e}_{j_m}^L\right) = \frac{1}{m!} \sum_{l_1,\ldots,l_m \in P_{\{j_1,\ldots,j_m\}}} \left(\mathbf{e}_{l_1}^L \otimes \cdots \otimes \mathbf{e}_{l_m}^L\right). \tag{15}$$

In addition, the intermediate matrix $\mathbf{G} \in \mathbb{R}^{L^m \times C_{L+m-1}^m}$ needs to be built. The columns of the matrix $\mathbf{G}$ can be defined as follows:

$$\left\{\pi_S\left(\mathbf{e}_{j_1}^L \otimes \ldots \otimes \mathbf{e}_{j_m}^L\right) : (j_1, \ldots, j_m) \in Q_L^m\right\}. \tag{16}$$

Furthermore, the matrix $\mathbf{W} = \mathbf{G}[\widehat{w}_1, \ldots, \widehat{w}_{C_R^{L-1}}]$ can be obtained. Reshape the $L^m \times C_R^{L-1}$ matrix $\mathbf{W}$ into an $L \times L^{m-1} \times C_R^{L-1}$ tensor $\mathscr{W}$. Afterwards, we need to compute the CPD of the tensor $\mathscr{W} = [\mathbf{F}, \mathbf{M}_1, \mathbf{M}_2]_{C_R^{L-1}}$ by generalized eigenvalue decomposition (GEVD). The tensor CPD procedure by GEVD is shown in [21].

3.2. Estimation of Factor Matrices. Once the tensor $\mathscr{W}$ is constructed, we can obtain the matrix unfoldings:

$$\begin{aligned} \mathbf{W}_{\mathscr{F}} &= \begin{bmatrix} \mathbf{W}_1 \\ \vdots \\ \mathbf{W}_{C_R^{L-1}} \end{bmatrix} = \begin{bmatrix} \mathbf{F}\mathrm{Diag}\left(\mathbf{m}_2^1\right)\mathbf{M}_1^T \\ \vdots \\ \mathbf{F}\mathrm{Diag}\left(\mathbf{m}_2^{C_R^{L-1}}\right)\mathbf{M}_1^T \end{bmatrix} \\ &= (\mathbf{M}_2 \odot \mathbf{F})\mathbf{M}_1^T, \end{aligned} \tag{17}$$

where $\mathbf{W}_{\mathscr{F}} \in \mathbb{C}^{LC_R^{L-1} \times L^{m-1}}$, $\mathbf{W}_{k'} = [w_{i'j'k'}]_{i',j'=1}^{L,L^{m-1}}$ symbolizes the k'th frontal slice of $\mathscr{W}$, $\mathbf{m}_2^i$ denotes the ith row of the $\mathbf{M}_2$, and $\mathrm{Diag}(\cdot)$ is the diagonalization operator. According to (17), the following equation can be easily derived:

$$\mathbf{W}_{k_1'}\mathbf{W}_{k_2'}^{\dagger} = \mathbf{F}\mathrm{Diag}\left(\mathbf{m}_2^{k_1'}\right)\mathrm{Diag}\left(\mathbf{m}_2^{k_2'}\right)^{-1}\mathbf{F}^{\dagger}, \tag{18}$$

where $k_1' \neq k_2'$, $k_1', k_2' = 1, \ldots, C_R^{L-1}$, and $(\cdot)^{\dagger}$ denotes the Moore–Penrose inverse. Obviously, the columns of the factor matrix $\mathbf{F}$ are the eigenvectors of $\mathbf{W}_{k_1'}\mathbf{W}_{k_2'}^{\dagger}$. The corresponding eigenvalues are the first C_R^{L-1} larger eigenvalues, which are arranged in a descending order. It is worth noting that when $C_R^{L-1} > 2$, there are multiple combinations (k_1', k_2') that can be used for EVD. In order to fully exert the statistical characteristics of (17), C_H^2 possible combinations are selected for EVD to obtain $\mathbf{F}_{h'}$, where $h' = 1, \ldots, C_H^2$, $H = C_R^{L-1}$. Herein, we make the agreement that (k_1', k_2') tuples are ordered lexicographically: the h_1'th tuple (k_1', k_2') is preceding the h_2'th tuple (k_3', k_4') if and only if $k_1' \leq k_3'$ and $k_2' \leq k_4'$. According to the trivial indeterminacies aforementioned for CPD uniqueness, $\mathbf{F}_{h_1'}$ and $\mathbf{F}_{h_2'}$ coincide up to column permutation and scaling, $h_1' \neq h_2'$. Therefore, we need to match multiple sets of results; i.e., all the eigenvectors need to be normalized and arranged in a descending order according to the corresponding eigenvalues. The results of the matching processing are recorded as $\mathbf{F}_{h'}'$, and the estimation of the factor matrix $\mathbf{F}$ can be obtained by performing the following statistical operation:

$$\mathbf{F} = \frac{1}{C_H^2} \sum_{h'=1}^{C_H^2} \mathbf{F}_{h'}'. \tag{19}$$

Once the matrix $\mathbf{F}$ is obtained, we can recover the matrix $\mathbf{B}$ from $\mathbf{F}$. First, compute R submatrices $\mathbf{F}_1, \ldots, \mathbf{F}_R$ of C_{R-1}^{L-2} columns of $\mathbf{F}$ that are linearly dependent. Then, compute $\mathbf{b}_1, \ldots, \mathbf{b}_R$ as orthogonal complements to the submatrices aforementioned. It is worth noting that, in the presence of noise, the algorithm proposed in this paper only guarantees that $\|\mathbf{b}_r\mathbf{F}_r\|_2 \leq 10^{-15}$. Furthermore, the factor matrices $\mathbf{A}$ and $\mathbf{C}$ can be recovered, thanks to $\mathbf{R}_{1,0}(\mathscr{Y})\mathbf{B}^{-T} = \mathbf{A} \odot \mathbf{C}$.

3.3. Estimation of Signal Parameters. The construction of the factor matrices clearly shows that the factor matrix $\mathbf{A}$ contains the spatial-polarization parameters of the signals, while the factor matrix $\mathbf{B}$ includes only the spatial ones of them. Putting it in other way, $\mathbf{a}_r$ and $\mathbf{b}_r$ are the estimated counterparts of $\mathbf{a}^p(\Psi_r)$ and $\mathbf{a}^s(\theta_r, \phi_r)$, respectively. Thus, the following equations are going to be used to obtain the spatial DOA of the rth signal impinging on the array:

$$\left[\mathbf{b}_r\right]_1 = e^{-i2\pi\left(\mathbf{b}_1^T\epsilon_{\mathbf{r}}/\lambda\right)}, \ldots, \left[\mathbf{b}_r\right]_L = e^{-i2\pi\left(\mathbf{b}_L^T\epsilon_{\mathbf{r}}/\lambda\right)}. \tag{20}$$

It is obvious that the DOA of the rth signal can be procured through any two equations from (20). Suppose $(\theta_r, \phi_r)_n$ is the representation of the nth subequations' solution. Under such circumstances, the DOA can be estimated through the average of multiple sets' solutions:

$$(\theta_r, \phi_r) = \frac{1}{C_L^2} \sum_{n=1}^{C_L^2} (\theta_r, \phi_r)_n. \tag{21}$$

Once the DOA is estimated, a further step is taken to extract the polarization parameters (γ_r, η_r) of the rth signal from the following formula:

$$\mathbf{a}_r = \mathscr{B}\Xi_{\theta_r,\phi_r}\left[\cos\gamma_r,\ \sin\gamma_r e^{i\eta_r}\right]^T. \tag{22}$$

In order to simplify the decomposition of the tensor-based signal model, the value of the snapshots K is supposed to be as small as possible when $K \geq R$ is satisfied. Therefore, we take N-segment K snapshots to improve the estimation accuracy of signal parameters. That is, the signal parameters which are estimated through decomposing over N times are going to be averaged.

4. Simulation Results

Consider a uniform linear array (ULA) with 4 complete EM vector sensors whose spacing is half wavelength. Suppose there are three signals with the polarization

parameters $(\gamma_1, \eta_1) = (20^\circ, 90^\circ)$, $(\gamma_2, \eta_2) = (45^\circ, 90^\circ)$, and $(\gamma_3, \eta_3) = (60^\circ, 90^\circ)$ impinging on the ULA from $(\theta_1, \phi_1) = (30^\circ, 90^\circ)$, $(\theta_2, \phi_2) = (10^\circ, 90^\circ)$, and $(\theta_3, \phi_3) = (60^\circ, 90^\circ)$, respectively. s_1 is independent of s_2, and s_3 is the replica of s_2, which means that there is a coherency between s_2 and s_3. All of the signals have the same power. In addition, the noise component is assumed to be zero-mean additive white Gaussian noise. The root mean square error (RMSE) is defined as

$$\mathrm{RMSE}(\mu) = \sqrt{\frac{1}{MR}\sum_{m=1}^{M}\sum_{r=1}^{R}\left(\widehat{\mu}_{rm} - \mu_r\right)^2}, \tag{23}$$

where M is the Monte Carlo trial number, μ_r denotes one of the parameters $(\theta_r, \phi_r, \gamma_r, \eta_r)$, and $\widehat{\mu}_{rm}$ is the estimation of μ_r in the mth trial.

The DOA estimation of the signals at SNR = 20 dB with 10 independent trials is illustrated in Figure 1. As expected, our proposed algorithm succeeds in differentiating the signals without paying special attention to their coherency.

For all the following simulations, their results derive from 300 Monte Carlo trials and have been compared with the Cramér–Rao lower bound (CRB) benchmark which is described in Appendix C.

In Figure 2, the proposed algorithm is compared with two advanced subspace-based algorithms in terms of the RMSE versus number of snapshots for SNR = 20 dB. It can be seen from Figure 2 that the DOA estimation accuracy of the proposed algorithm outperforms the other two algorithms. Especially for the case of fewer number of snapshots, the advantages of the proposed algorithm are obvious.

Figure 3 illustrates the superior performance of the proposed algorithm as compared to the other two algorithms when the snapshots number is set as 200. It is worth noting that as SNR increases, the tensor-based methods, i.e., the proposed algorithm and the HOSVD-based algorithm, present a better accuracy of the DOA estimation than the Toeplitz-based algorithm. What is more, the estimation performance of the polarization parameters is examined in Figure 4, which is conducted under the same scenarios with those in Figure 3. According to the operation process mentioned above, we know that, in the proposed algorithm, polarization parameters cannot be estimated independently without obtaining the DOA estimation because the estimation of polarization parameters can only be achieved with the predicted DOA at hand at first. When comparing Figure 4 with Figure 3, we can see clearly that the estimation accuracy of polarization parameters is inferior to that of DOA parameters, and the reason lies in the accumulation of the estimation error during these two steps. Nevertheless, the estimation accuracy of polarization parameters in the proposed algorithm is still better than that of the other two algorithms.

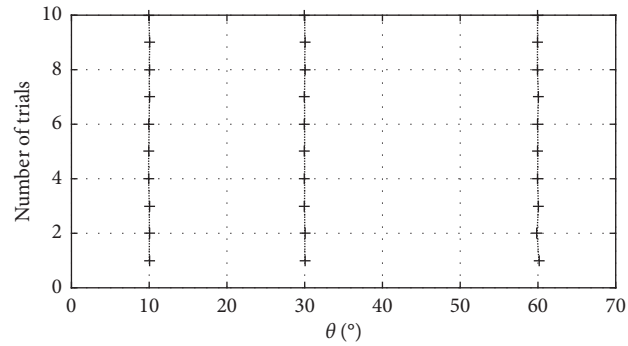

Figure 1: DOA estimation of the signals with the proposed algorithm at SNR = 20 dB.

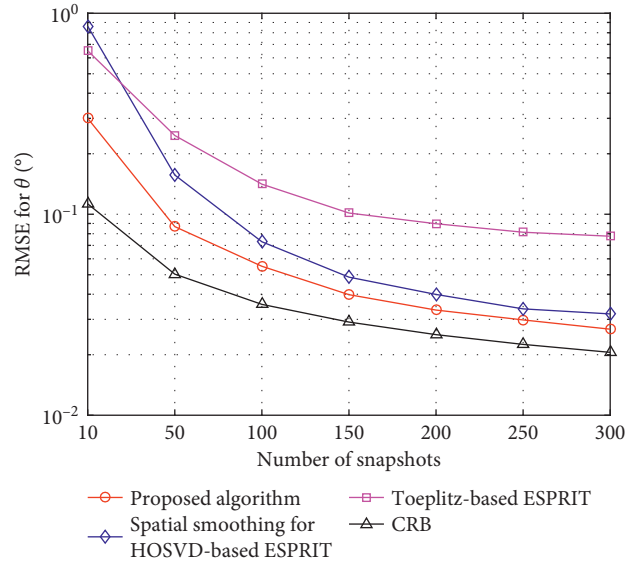

Figure 2: DOA RMSE versus number of snapshots for SNR = 20 dB.

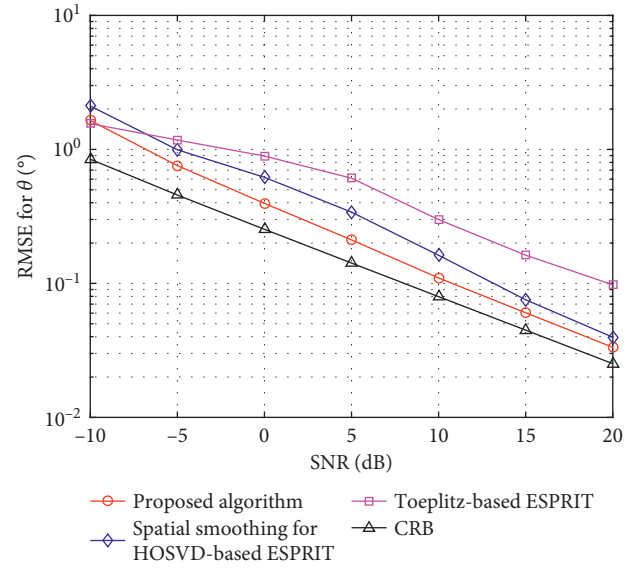

Figure 3: DOA RMSE versus SNR for NK = 200.

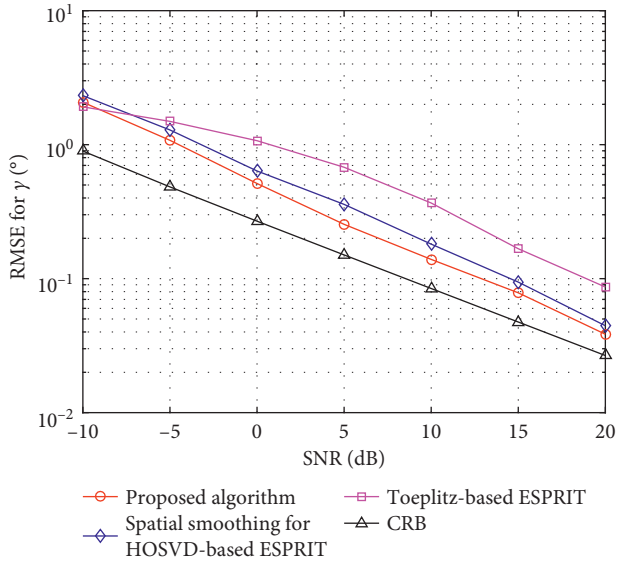

Figure 4: Polarization parameter's RMSE versus SNR for NK = 200.

5. Conclusions

With the purpose of surmounting the problem of parameter estimation for coherent signals, this paper proposes a new approach which features decomposition for tensors. Specifically, factor matrices can be effectively estimated at first and then be used to extract the parameters of signals irrespective of the coherency between them. In view of this, an obvious advantage of this approach lies in its effective estimation of factor matrices even with noises present. Besides, the problem of aperture loss, which commonly appears in most traditional algorithms, can also be avoided under this approach. Meanwhile, according to the simulation results, our proposed algorithm shows a higher accuracy of parameter estimation in comparison with the state-of-the-art ones.

Appendix

A. Construction of the Intermediate Matrix

Let $P_{\{i_1,\dots,i_k\}}$ serve as the indication of the set of all permutations of the set $\{i_1,\dots,i_k\}$. It is important to note that the cardinality of $P_{\{i_1,\dots,i_k\}}$ is counted by considering multiplicities (e.g., $P_{\{1,1,1\}}$ is made up of six identical entries $(1,1,1)$) if some of the values coincide.

It is easy to know that any integer from $\{1,\dots,J^{m+i}L^{m+i}\}$ can be uniquely denoted as $(\widetilde{j}-1)L^{m+i}+\widetilde{l}$ and any integer from $\{1,\dots,K^{m+i}\}$ as $\widetilde{k}$, where

$$\begin{aligned}\widetilde{j} &:= 1+\sum_{p=1}^{m+i}\left(j_p-1\right)J^{m+i-p},\\ \widetilde{l} &:= 1+\sum_{p=1}^{m+i}\left(l_p-1\right)L^{m+i-p},\\ \widetilde{k} &:= 1+\sum_{p=1}^{m+i}\left(k_p-1\right)K^{m+i-p},\end{aligned} \tag{A.1}$$

and $j_1,\dots,j_{m+i}\in\{1,\dots,J\}$, $l_1,\dots,l_{m+i}\in\{1,\dots,L\}$, and $k_1,\dots,k_{m+i}\in\{1,\dots,K\}$. These equations are of great use if there is going to have a switch between tensor, matrix, and vector indications. Hereinto, the $((\widetilde{j}-1)L^{m+i}+\widetilde{l},\widetilde{k})$th entry of the $L^{m+i}J^{m+i}\times K^{m+i}$ matrix $\mathbf{R}_{m,i}(\mathcal{T})$ can be defined as follows:

$$\frac{1}{m!\,(m+i)!}\sum_{(s_1,\dots,s_{m+i})\in P_{\{k_1,\dots,k_{m+i}\}}}\det\begin{bmatrix} t_{j_1l_1s_1} & \cdots & t_{j_1l_ms_m}\\ \vdots & \vdots & \vdots\\ t_{j_ml_1s_1} & \cdots & t_{j_ml_ms_m}\end{bmatrix}\cdot\prod_{p=1}^{l}t_{j_{m+p}l_{m+p}s_{m+p}}. \tag{A.2}$$

B. Construction of the Compound Matrix

The m-th compound matrix of a given matrix is derived from $m\times m$ minors of that matrix. Let $\mathbf{X}\in\mathbb{C}^{J\times K}$. The $C_J^m\times C_K^m$ matrix whose (a,b)-th entry is $\det\mathbf{X}(S_J^m(a),S_K^m(b))$ is called the m-th compound matrix of $\mathbf{X}$ and is represented by $\mathscr{C}_m(\mathbf{X})$, where $m\le\min(J,K)$. Let $i_1,\dots,i_k$ represent integers. The multi-index notation S_n^m can be defined as

$$S_n^m=\{(i_1,\dots,i_k):1\le i_1<i_2<\cdots<i_k\le n\}. \tag{A.3}$$

We assume that the elements of S_n^m are ordered lexicographically. It is well known that $S_3^2=\{(1,2),(1,3),(2,3)\}$. For example, let $\mathbf{X}=[\mathbf{I}_2,\mathbf{a}]$, where $\mathbf{a}=[a_1,a_2]^T$. Then,

$$\begin{aligned}\mathscr{C}_2(\mathbf{X}) &= \begin{bmatrix}\begin{vmatrix}1&0\\0&1\end{vmatrix} & \begin{vmatrix}1&a_1\\0&a_2\end{vmatrix} & \begin{vmatrix}0&a_1\\1&a_2\end{vmatrix}\end{bmatrix}\\ &= [1,a_2,-a_1].\end{aligned} \tag{A.4}$$

It is well known that $\mathscr{C}_m(\mathbf{X}^T)=(\mathscr{C}_m(\mathbf{X}))^T$ and $\mathscr{C}_m(\mathbf{X})$ is equal to the zero matrix if and only if $m>r_{\mathbf{X}}$.

C. Cramér–Rao Lower Bound for the Vector Sensor Array

The following matrix form is established after considering the situations described in (6):

$$\mathbf{y}(k)=\mathbf{A}\mathbf{s}(k)+\mathbf{n}(k), \tag{A.5}$$

in which $\mathbf{A}=[\mathbf{a}(\Psi_1)\dots\mathbf{a}(\Psi_R)]\in\mathbb{C}^{LJ\times R}$ and $\mathbf{s}(k)=[s_1(k)\dots s_R(k)]^T\in\mathbb{C}^{R\times 1}$. $\mathbf{\Psi}=[\Psi_1,\dots,\Psi_R]^T$ represents the unknown parameters vector, where Ψ_r serves as an indication of the unknown parameters vector of the rth source, $r\in[1,\dots,R]$. The matrix $\mathbf{A}$ in (A.5) is assumed to be column full rank so is the Jacobian $\partial\mathbf{A}/\partial\mathbf{\Psi}$. On the basis of this, we further set

$$\begin{aligned}\widetilde{A} &= \left[\widetilde{\mathbf{a}}_1^{(1)},\dots,\widetilde{\mathbf{a}}_{q_1}^{(1)},\dots,\widetilde{\mathbf{a}}_1^{(R)},\dots,\widetilde{\mathbf{a}}_{q_R}^{(R)}\right],\\ \widetilde{\mathbf{a}}_m^{(n)} &= \frac{\partial\mathbf{a}(\Psi_n)}{\partial\Psi_n(m)},\end{aligned} \tag{A.6}$$

where the number of elements in vector Ψ_r is represented by q_r. Exploring the performance of estimating $\boldsymbol{\Psi}$ in (A.5) from $\mathbf{x}(1), \ldots, \mathbf{x}(K)$ is our main concern in this paper.

The purpose of constructing the following two intermediate matrices lies in simplifying the expression of the Cramér–Rao lower bound mentioned before:

$$\begin{aligned} \mathbf{U} &= \mathbf{R}_{ss}\left(\mathbf{A}^H\mathbf{A}\mathbf{R}_{ss} + \sigma^2\mathbf{I}\right)^{-1}\mathbf{A}^H\mathbf{A}\mathbf{R}_{ss}, \\ \mathbf{P} &= \mathbf{I} - \mathbf{A}\left(\mathbf{A}^H\mathbf{A}\right)^{-1}\mathbf{A}^H, \end{aligned} \tag{A.7}$$

where $\mathbf{R}_{ss}$ represents the covariance of the signal matrix $\mathbf{S} = [\mathbf{s}(1), \ldots, \mathbf{s}(K)]$, σ^2 symbolizes the noise variance, and $\mathbf{I}$ serves as the denotation of a $R \times R$ unit matrix. For $\boldsymbol{\Psi}$, the Cramér–Rao lower bound of its unbiased estimation is

$$\mathbf{CRB}(\boldsymbol{\Psi}) = \frac{\sigma^2}{2K}\left\{\mathrm{Re}\left[\mathrm{btr}\left((1 \boxtimes \mathbf{U}) \boxdot \left(\widetilde{A}^H\mathbf{P}\widetilde{A}\right)^{bT}\right)\right]\right\}^{-1}, \tag{A.8}$$

where 1 is an indication of a $\overline{q} \times \overline{q}$ matrix with all entries equal to one, $\overline{q} = \sum_{r=1}^{R} q_r$. Assuming that the (i, j)-th block entry of the matrix $\mathbf{Q}$ is represented by $\mathbf{Q}_{\langle ij\rangle}$ with dimension $p_i \times p_j$, the block operators $\mathrm{btr}(\cdot)$, bT, $\boxtimes$, and $\boxdot$ are defined as follows.

Definition 1. Block trace operator:

$$[\mathrm{btr}(\mathbf{Q})]_{ij} = \mathrm{tr}\left(\mathbf{Q}_{\langle ij\rangle}\right). \tag{A.9}$$

Definition 2. Block transpose:

$$\left(\mathbf{Q}^{bT}\right)_{\langle ij\rangle} = \mathbf{Q}_{\langle ij\rangle}. \tag{A.10}$$

Definition 3. Block Kronecker product:

$$\left(\mathbf{Q}_1 \boxtimes \mathbf{Q}_2\right)_{\langle ij\rangle} = \left[\mathbf{Q}_1\right]_{\langle ij\rangle} \otimes \left[\mathbf{Q}_2\right]_{\langle ij\rangle}. \tag{A.11}$$

Definition 4. Block Hadamard product:

$$\left(\mathbf{Q}_1 \boxdot \mathbf{Q}_2\right)_{\langle ij\rangle} = \left[\mathbf{Q}_1\right]_{\langle ij\rangle}\left[\mathbf{Q}_2\right]_{\langle ij\rangle}. \tag{A.12}$$

Data Availability

The data used to support the findings of this study are available from the corresponding author upon request.

Conflicts of Interest

The authors declare that there are no conflicts of interest regarding the publication of this paper.

Acknowledgments

This work was supported by the National Natural Science Foundation of China under Grant nos. 61771404 and 61601372.

References

[1] S. U. Pillai and B. H. Kwon, "Forward/backward spatial smoothing techniques for coherent signal identification," *IEEE Transactions on Acoustics, Speech, and Signal Processing*, vol. 37, no. 1, pp. 8–15, 1989.

[2] W. Du and R. L. Kirlin, "Improved spatial smoothing techniques for DOA estimation of coherent signals," *IEEE Transactions on Signal Processing*, vol. 39, no. 5, pp. 1208–1210, 1991.

[3] J. Dai and Z. Ye, "Spatial smoothing for direction of arrival estimation of coherent signals in the presence of unknown mutual coupling," *IET Signal Processing*, vol. 5, no. 4, pp. 418–425, 2011.

[4] J. Wen, B. Liao, and C. Guo, "Spatial smoothing based methods for direction-of-arrival estimation of coherent signals in nonuniform noise," *Digital Signal Processing*, vol. 67, pp. 116–122, 2017.

[5] J. Shi, G. Hu, and X. Zhang, "Direction of arrival estimation in low-grazing angle: a partial spatial-differencing approach," *IEEE Access*, vol. 5, pp. 9973–9980, 2017.

[6] F. M. Han and X. D. Zhang, "An ESPRIT-like algorithm for coherent DOA estimation," *IEEE Antennas and Wireless Propaga Letters*, vol. 4, pp. 443–446, 2005.

[7] X. Zhang and D. Xu, "Improved coherent DOA estimation algorithm for uniform linear arrays," *International Journal of Electronics*, vol. 96, no. 2, pp. 213–222, 2009.

[8] Y.-H. Choi, "ESPRIT-Based coherent source localization with forward and backward vectors," *IEEE Transactions on Signal Processing*, vol. 58, no. 12, pp. 6416–6420, 2010.

[9] C. Li, G. Liao, S. Zhu, and S. Wu, "An ESPRIT-like algorithm for coherent DOA estimation based on data matrix decomposition in MIMO radar," *Signal Processing*, vol. 91, no. 8, pp. 1803–1811, 2011.

[10] A. Goian, M. I. AlHajri, R. M. Shubair et al., "Fast detection of coherent signals using pre-conditioned root-MUSIC based on Toeplitz matrix reconstruction," in *Proceedings of the IEEE 11th International Conference on Wireless and Mobile Computing, Networking and Communications*, pp. 168–174, Abu Dhabi, UAE, October 2015.

[11] J. Li, Q.-H. Lin, C.-Y. Kang, K. Wang, and X.-T. Yang, "DOA estimation for underwater wideband weak targets based on coherent signal subspace and compressed sensing," *Sensors*, vol. 18, no. 3, p. 902, 2018.

[12] D. Li, M. Zhan, J. Su, H. Liu, X. Zhang, and G. Liao, "Performances analysis of coherently integrated CPF for LFM signal under low SNR and its application to ground moving target imaging," *IEEE Transactions on Geoscience and Remote Sensing*, vol. 55, no. 11, pp. 6402–6419, 2017.

[13] M. Haardt, F. Roemer, and G. Del Galdo, "Higher-order SVD-based subspace estimation to improve the parameter estimation accuracy in multidimensional harmonic retrieval problems," *IEEE Transactions on Signal Processing*, vol. 56, no. 7, pp. 3198–3213, 2008.

[14] M. Boizard, G. Ginolhac, F. Pascal, S. Miron, and P. Forster, "Numerical performance of a tensor MUSIC algorithm based on HOSVD for a mixture of polarized sources," in *Proceedings of the 21st European Signal Processing Conference (EUSIPCO 2013)*, pp. 1–5, Marrakech, Morocco, September 2013.

[15] K. Han and A. Nehorai, "Nested vector-sensor array processing via tensor modeling," *IEEE Transactions on Signal Processing*, vol. 62, no. 10, pp. 2542–2553, 2014.

[16] P. Forster, G. Ginolhac, and M. Boizard, "Derivation of the theoretical performance of a tensor MUSIC algorithm," *Signal Processing*, vol. 129, pp. 97–105, 2016.

[17] X. Lan, L. Wang, Y. Wang, C. Choi, and D. Choi, "Tensor 2-D DOA estimation for a cylindrical conformal antenna array in a massive MIMO system under unknown mutual coupling," *IEEE Access*, vol. 6, pp. 7864–7871, 2018.

[18] X. J. Guo, S. Miron, D. Brie, S. H. Zhu, and X. W. Liao, "A CANDECOMP/PARAFAC perspective on uniqueness of DOA estimation using a vector sensor array," *IEEE Transactions on Signal Processing*, vol. 59, no. 7, pp. 3475–3481, 2011.

[19] F. Raimondi, P. Comon, O. Michel, S. Sahnoun, and A. Helmstetter, "Tensor decomposition exploiting diversity of propagation velocities: application to localization of icequake events," *Signal Processing*, vol. 118, pp. 75–88, 2016.

[20] L. Liu, L. Wang, and Z. Zhang, "Vector-sensor-based signal parameter estimation by exploiting CPD of tensors," *IEEE Sensors Letters*, vol. 2, no. 3, pp. 1–4, 2018.

[21] L. Liu, L. Wang, J. Xie, and Z. L. Zhang, "DOA and polarization parameters estimation by exploiting canonical polyadic decomposition of tensors," *Wireless Communications and Mobile Computing*, vol. 2019, Article ID 7389306, 12 pages, 2019.

[22] I. Domanov and L. De Lathauwer, "Canonical polyadic decomposition of third-order tensors: relaxed uniqueness conditions and algebraic algorithm," *Linear Algebra and its Applications*, vol. 513, pp. 342–375, 2017.

[23] I. Domanov and L. D. Lathauwer, "Canonical polyadic decomposition of third-order tensors: reduction to generalized eigenvalue decomposition," *SIAM Journal on Matrix Analysis and Applications*, vol. 35, no. 2, pp. 636–660, 2014.